DETERMINATION OF DISTRIBUTION OF HEAT-CONDUCTING MATERIAL CONCENTRATION IN PROTECTIVE LAYER OF THERMAL PROTECTION SYSTEM PANEL

by

***Lukasz BRODZIK** and Andrzej FRACKOWIAK**

Chair of Thermal Engineering, Poznan University of Technology,
Poznan, Poland

Original scientific paper
https://doi.org/10.2298/TSCI19S4025B

Paper presents the problem of heating the damaged insulation of an orbiter. Changes of the insulation's thermal properties, made by adding conductive material of high value of specific heat in a form of a dope to the protective layer, were examined. An iterative algorithm determining a variable of dope concentration in the material was developed. Insulating material LI900 was used for calculations. Determination of distribution of conductive material concentration was made for materials which, after verification, demonstrated the most beneficial effect on protective properties of the modified insulation layer. Change of properties was to enable time extension of the LI900 insulation tile heating up to the maximal temperature and, additionally, to lowering this temperature.

Keywords: *thermal protection system, heat conduction, porous material thermal radiation, aerodynamic heating, numerical analysis*

Introduction

The problems of heating of thermal shields of orbiters usually focus on two important topics:

- evaluation of the existing reusable thermal protection system and
- search for new solutions of the said system.

The first of the two problems is discussed in literature concentrating on the insulation itself, its thermal loads and the influence of damage on the load endurance [1, 2]. There are results of experimental research that show how the insulation heats up in different gas environments [3], and how it can be used in spaceflights [4]. To this end, the possibility of a combination of the insulator and the ablator has been explored. In such a combination, the ablator serves its purpose only in the initial stage of the heating during atmospheric reentry, when the temperatures are too high for a modern reusable heat protection system.

The second of the problems is discussed in works [5, 6]. The literature is very often devoted to the shields designed based on metal alloys *e. g.* honeycomb shaped structures [7, 8]. The advantage of such solutions is a significant increase in the durability and resistance to impact. Despite the resistance to relatively high thermal loads, they still have great limitations compared to insulation. The idea of applying MHD power panels appears to be very interest-

* Corresponding author, e-mail: lukasz.brodzik@put.poznan.pl

ing [9]. It consists in using the external source of power (from the hot air around the orbiter). The sudden surge in the power output can be used to activate the thermal shield.

Unfortunately, there are few publications that present the thermos mechanical analysis of damaged surface insulation. Besides, the solutions of this problem in recent literature findings either do not contain data related to the properties of the used materials or their efficiency is still to be confirmed experimentally. The LI900 surface insulation is a well-explored material, and much information can be obtained about it [10-12]. The material is reliable, which makes it appropriate in terms of research on the advancement of the existing thermal protection systems.

The object of the research described in this paper is high temperature reusable surface insulation (HRSI) of an orbiter. In extreme cases, the damage of the insulation material results in melting of the orbiter aluminum structure, leading directly to its destruction. Under normal conditions, when the thermal protection system is fully operative, a significant increase in the temperature of the orbiter structure takes place only after the vehicle has landed. When a malfunction occurs, the temperature increase takes place earlier, already at the flight stage. Contrary to many concepts discussed in literature, the paper does not focus on increasing of the thermal durability.

Formulation of the heat transfer problem

The numerical simulations were carried out in the FreeFem++ environment with the assumed flight duration of the shuttle of t_2 = 2100 s and the present heat flux, fig. 1. Each model used in the research had 3 layers, *i. e.* aluminum structure of the vehicle (1.6002 mm thick), NOMEX SIP (4.3942 mm thick), and the LI900 insulation (77 mm thick), fig. 2.

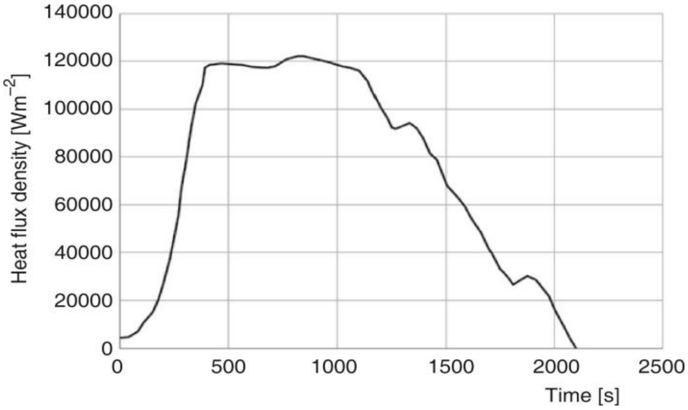

Figure 1. Distribution of heat flux density as a function of time [2]

The conductive material in the insulation was nickel, beryllium, and a material of ideal thermal parameters (reference material). The specifications of the HRSI tile material and additional materials were taken from [13]. For the reference material, the material data of hydrogen were adopted. Due to its very large value of specific heat, it expresses the theoretical limit of the possibilities in the presented method. Material properties of dopant are presents in tab. 1.

Model of damage was made for the case, where the defect in insulation is formed by an impact with small object moving at a hypersonic speed. Its shape and simplification is given in fig. 3. In the simulations were included models 1, 2, 3, 4, and 5 for which the following diameter D equal to 0, 1, 2, 3, and 4 cm.

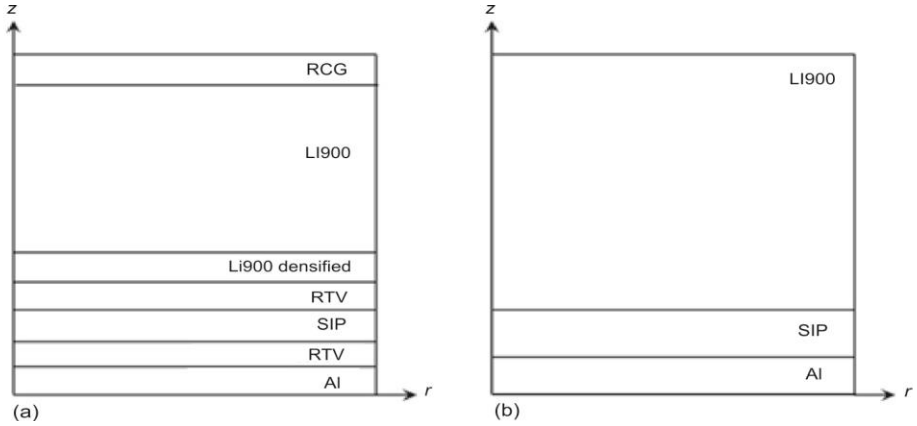

Figure 2. Geometry of model; (a) the real model, (b) simplification

Table 1. Material properties of additional materials

T [°C]	c_p [Jkg^{-1}K^{-1}]	k [Wm^{-1}K^{-1}]	ρ [kgm^{-3}]	Material
20	444	90,0	8902	nickel
20	1825	218	1848	beryllium
20	10000	10	1000	reference material

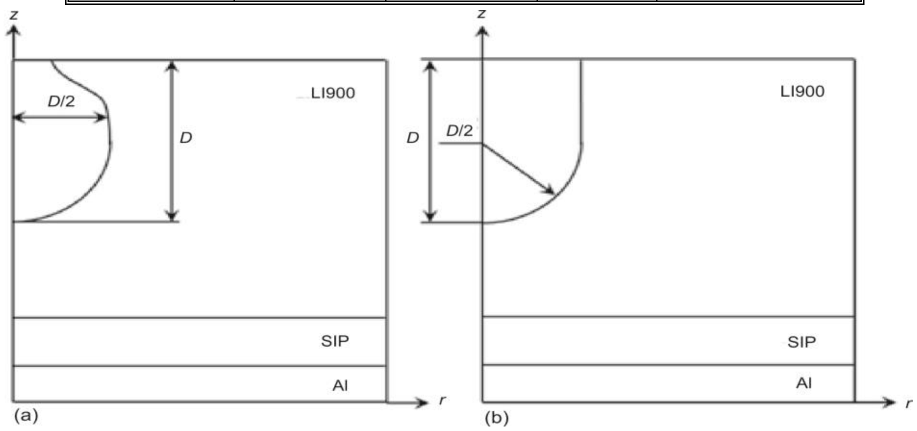

Figure 3. Geometry of damage; (a) the real model, (b) simplification

Problem of radiation was solved using P1 approximation. This model assumes plane-parallel symmetry that matter is in local thermodynamic equilibrium, scattering is coherent and isotropic. This model is one of approximations to solve radiative transfer equation. This equation for an absorbing, emitting, and scattering medium at position $\vec{R}$ in the direction $\vec{s}$ is [14, 15] , fig. 4:

$$\frac{\mathrm{d}I\left(\vec{R},\vec{s}\right)}{\mathrm{d}s} = -\beta I\left(\vec{R},\vec{s}\right) + \kappa_a n^2 \frac{\sigma T^4}{\pi} + \frac{\kappa_s}{4\pi}\int_0^{4\pi} I\left(\vec{R}',\vec{s}\right) P\left(\vec{R},\vec{R}'\right)\mathrm{d}\vec{R}' \qquad (1)$$

where $\vec{R} \in \Omega_2$, $I\left(\vec{R},\vec{s}\right)$ is the intensity of radiation, $P\left(\vec{R},\vec{R}'\right)$ – the phase function, and $\vec{R}'$ – the direction of displacement of photon as a result of scattering.

In the literature about radiation transport problem may find works, which shows that results gave by P1 approximation are comparable with results obtained using Monte Carlo method [16, 17]. The First law of thermodynamics and Fourier’s law were used in carrying out the analysis of the heat-flow in non-stationary conditions for axisymmetric heat conduction model. Therefore, for the cylindrical co-ordinate system in space, Ω_1, the following formula was used:

$$\rho c_p \left(\frac{\partial T}{\partial t}\right) = \frac{1}{r}\frac{\partial}{\partial r}\left(k_r r \frac{\partial T}{\partial r}\right) + \frac{\partial}{\partial z}\left(k_z \frac{\partial T}{\partial z}\right) \tag{2}$$

Initial condition is:

$$T|_{\Omega_1} = T_0 \tag{3}$$

where T_0 is initial temperature.

The model was built from three layers: underlying structure, strain isolator pad, and insulation. Space Ω_1 was defined by equation:

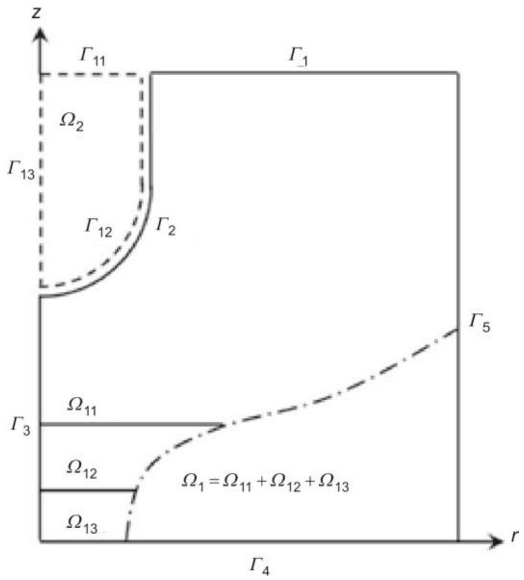

Figure 4. Layer numbering

$$\Omega_1 = \Omega_{11} + \Omega_{12} + \Omega_{13} \tag{4}$$

The cavity is filled by air that permanently flows through this space. Therefore, the heat is permanently being transported away from the cavity so the heat sources that can produce heat radiation are not present on the right-hand side of the eq. (4). Damage was represented by space Ω_2. In this part heat transfer was expressed by energy of the heat radiation φ and coefficient β:

$$\Delta\varphi - 3\beta^2\varphi = 0 \tag{5}$$

There was assumed that our hypothetical medium is homogeneous and isotropic, so it is characterized by the attenuation factor β only. Thus, this is a single fitting parameter and its value is reverse of the mean free path of photons in the medium. Boundary condition on the wall Γ_{12}:

$$\frac{\partial\varphi}{\partial n} = \frac{3\beta}{2}\frac{\varepsilon}{2-\varepsilon}\left[4\sigma\left(T_\mathrm{w}^4 - T_\mathrm{f}^4\right) - \varphi\right] \tag{6}$$

The condition on the boundary Γ_{11} was chosen:

$$\frac{\partial\varphi}{\partial n} = -\frac{3\beta}{2}\varphi \tag{7}$$

The boundary condition for Γ on the boundary Γ_2 was set:

$$-k\frac{\partial T}{\partial n} = -\left[q - \frac{1}{6\beta}\frac{\partial\varphi}{\partial n}\right] = -\left[q + \frac{1}{4}\frac{\varepsilon}{2-\varepsilon}\varphi - \frac{\varepsilon}{2-\varepsilon}\sigma\left(T_\mathrm{w}^4 - T_\mathrm{f}^4\right)\right] \tag{8}$$

For wall Γ_1 boundary condition is expressed:

$$-k\frac{\partial T}{\partial n} = -q + \varepsilon\sigma\left(T_{\mathrm{w}}^4 - T_{\mathrm{f}}^4\right) \tag{9}$$

In analysis convection was not considered, because it is very small. For walls Γ_3, Γ_4, and Γ_5 boundary condition:

$$\frac{\partial T}{\partial n} = 0 \tag{10}$$

For wall Γ_{13} boundary condition (symmetry):

$$\frac{\partial \varphi}{\partial n} = 0 \tag{11}$$

On the other hand, the motion of the medium in the cavity has no effect on the propagation of the heat radiation, and was applied conventional models of radiative heat transfer [15].

Problem of thermal conductivity of the additional material

The concentration of heat-conducting material, γ, in the insulating layer is defined in dimensionless co-ordinates, according to the indications from fig. 5:

$$\gamma = ab \tag{12}$$

Assuming $s = b/a$, dimensions of the conductive layer are:

$$a = \sqrt{\frac{\gamma}{s}}, \quad b = \sqrt{\gamma s} \tag{13}$$

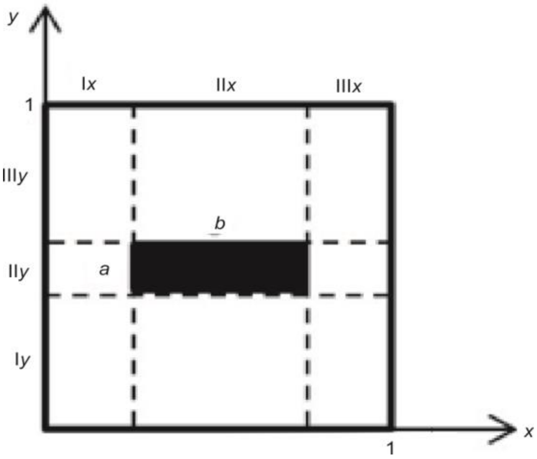

Figure 5. Location of the conductive layer inside the insulating layer in the elementary volume unit of material LI900

The heat capacity of the LI900 insulating layer with dopant of heat conductor filings is given:

$$\rho c = (\rho c)_{\mathrm{LI}}(1-\gamma) + (\rho c)_p \gamma \tag{14}$$

To estimate values of the equivalent conductivity coefficient separately in the direction of the x and y axes, the area of the square with side 1 is divided into three parts, fig. 4. Thermal conductivity of the insulating layer was marked as $k_{\mathrm{LI}x}$, $k_{\mathrm{LI}y}$ and the conductive layer as k_p. The thermal conductivities of layers Ix, IIx, IIIx are, respectively:

$$\begin{aligned} &\mathrm{I}x: && k_{\mathrm{LI}x} \\ &\mathrm{II}x: && \frac{k_{\mathrm{LI}x}k_p}{k_{\mathrm{LI}x}b + k_p(1-b)} \\ &\mathrm{III}x: && k_{\mathrm{LI}x} \end{aligned} \tag{15}$$

the equivalent thermal conductivity coefficient in the x-direction is equal:

$$k_x = (1-a)k_{\mathrm{LI}x} + a\frac{k_{\mathrm{LI}x}k_p}{k_{\mathrm{LI}x}b + k_p(1-b)}$$
$$k_x = \left(1-\sqrt{\frac{\gamma}{s}}\right)k_{\mathrm{LI}x} + \sqrt{\frac{\gamma}{s}}\frac{k_{\mathrm{LI}x}k_p}{k_{\mathrm{LI}x}\sqrt{\gamma s} + k_p\left(1-\sqrt{\gamma s}\right)} \tag{16}$$

Similarly, the equivalent thermal conductivity coefficient in the direction of the *y* axis was determined:

$$\begin{aligned} &\mathrm{I}y: \quad k_{\mathrm{LI}y} \\ &\mathrm{II}y: \quad \frac{k_{\mathrm{LI}y}k_p}{k_{\mathrm{LI}y}a + k_p(1-a)} \\ &\mathrm{III}y: \quad k_{\mathrm{LI}y} \end{aligned} \tag{17}$$

$$k_y = (1-b)k_{\mathrm{LI}y} + b\frac{k_{\mathrm{LI}y}k_p}{k_{\mathrm{LI}y}a + k_p(1-a)}$$
$$k_y = k_{\mathrm{LI}y} + \gamma k_{\mathrm{LI}y}\frac{1-\dfrac{k_{\mathrm{LI}y}}{k_p}}{1-a\left(1-\dfrac{k_{\mathrm{LI}y}}{k_p}\right)} \tag{18}$$

The filings are elongated in a transverse direction in relation to the main direction of the heat-flow. The heat conduction will mainly occur in the lateral direction of the insulation. In the paper, the influence of taking into account the conductivity of filings in the heat exchange in the vertical direction was checked. Using the previously discussed assumptions (for model of damaged tile, $D = 4$ cm), the analysis of the heat-flow through the insulator was performed. In the first case, calculations were made using the equivalent thermal conduction coefficient in the vertical and horizontal direction, eqs. (16) and (18). In the second case, only the equivalent thermal conduction coefficient was used in the horizontal direction, eq. (16). The temperature difference on the aluminum surface is shown in fig. 6. From the presented analysis, it can be concluded that in the calculations of heat exchange, the influence of changes in thermal conductivity of the insulator layer due to the presence of conductive material in the vertical direction can be neglected.

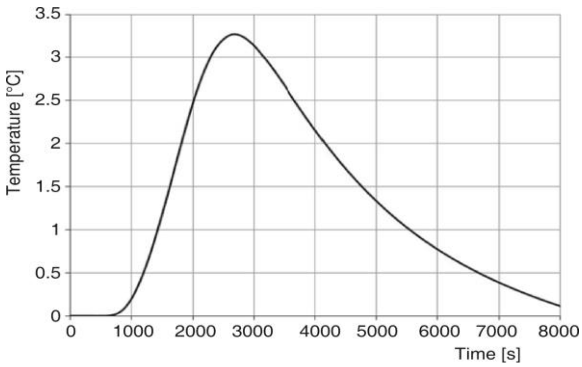

Figure 6. The difference between the maximum temperatures on the aluminum surface

Numerical analysis of the influence of conductive material concentration variable

In calculations for a model of a HRSI tile with an addition of nickel and the reference material, 1% and 3%, respectively, were made. The purpose of the iterative algorithm was to determine such a distribution of the concentration as to reduce the temperature increase on the surface of the aluminum structure. This objective was completed in all investigated cases, as shown in fig. 7. Significant differences occur among the curves of these cases after 2100 seconds. The most important factor decisive of whether the addition of the conductive material will serve its purpose in the insulation is its impact on the temperature curve of a damaged layer. In the investigations, a material loss of the diameter of 4 cm was assumed. These curves have been shown in fig. 8. In ideal conditions, with the 3% addition of reference material, due to its very high thermal capacity, the temperature in the structure was reduced by over 200 ºC. It is noteworthy, however, that the influence of the weight on the costs of operation in orbital transport is significant, which is why the temperature curve for the 1% addition of nickel may be more significant in practice.

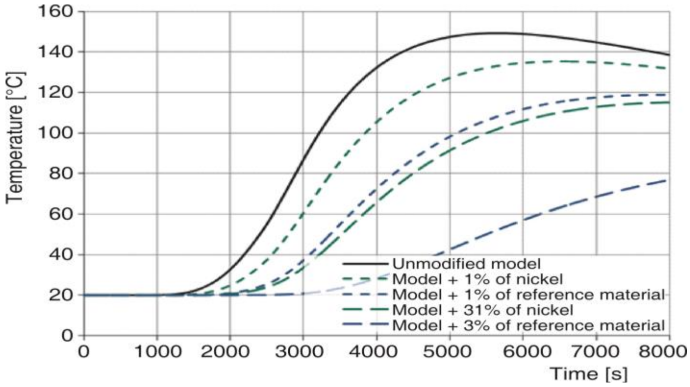

Figure 7. Comparison of the distribution of temperature on the surface of the orbiter structure for an undamaged tile
(*for colour image see journal web site*)

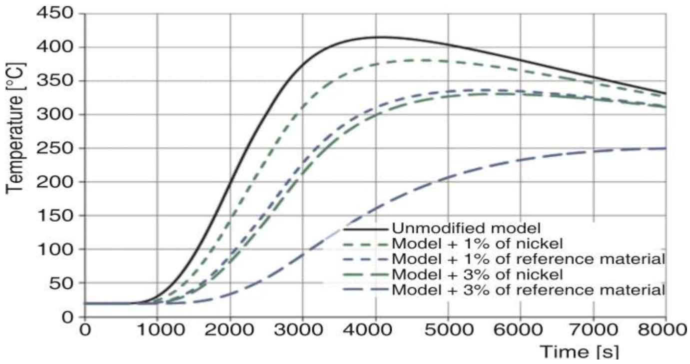

Figure 8. Comparison of the distribution of temperature on the surface of the orbiter structure for a damaged tile
(*for colour image see journal web site*)

It is noteworthy that in the performed analysis, after 2100 second from the atmospheric re-entry, the temperature of the structure with the 1% addition of nickel amounts to almost 150 ºC. The temperature of the aluminum structure without the addition after the same time is higher by approximatly 50 ºC. This is a very significant difference, because at the moment of the orbiter touchdown, the temperature of the aluminum alloy still remains within its admissible operating range. An additional conductive layer provides a more even heat transfer, fig. 9. Beryllium was also used as an admixture. The reason for this are its good thermal properties and, at the same time, low weight. The study indicates that there are no large differences in temperature distributions in models containing beryllium and nickel, fig. 10. The use of beryllium instead of nickel causes that the greater damage of insulation, the maximum temperature is higher, and the difference in its appearance decreases, tab. 2.

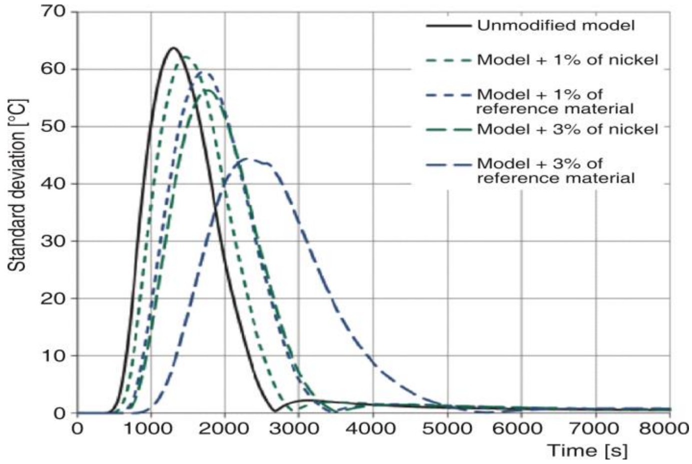

Figure 9. Standard deviation of temperature on the surface of SIP as a function of time – damaged tile model
(*for colour image see journal web site*)

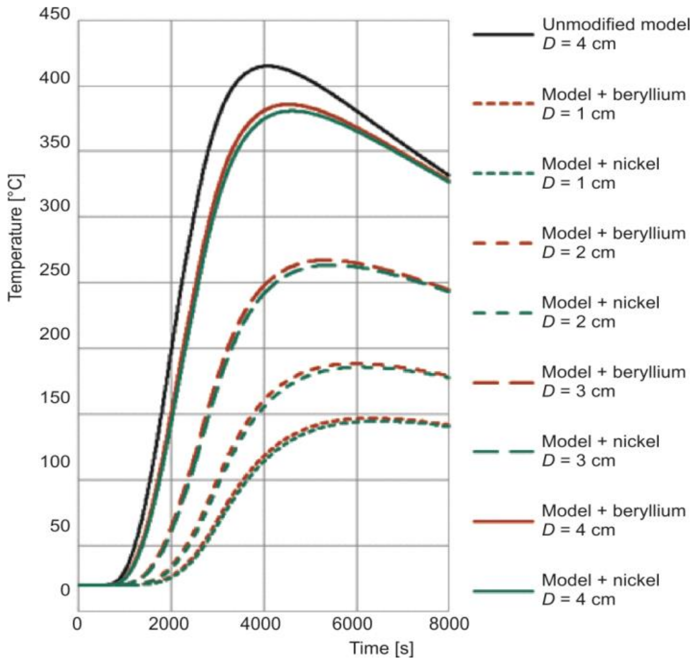

Figure 10. Comparison of the distribution of temperature on the surface of the orbiter structure for a damaged tile with light and heavy metallic dopant, γ = 1%
(*for colour image see journal web site*)

Table 2. Maximum temperature on the surface of the vehicle structure

Name of model	Temperature [°C]	Difference in temperature [°C]	Time [s]	Difference in time [s]
Undamaged model, *D* = 4 cm	415	–	4080	–
Model + beryllium, *D* = 1 cm	147	2	6305	140
Model + nickel, *D* = 1 cm	145		6445	
Model + beryllium, *D* = 2 cm	188	2	5975	140
Model + nickel, *D* = 2 cm	186		6095	
Model + beryllium, *D* = 3 cm	267	3	5350	105
Model + nickel, *D* = 3 cm	264		5455	
Model + beryllium, *D* = 4 cm	386	3	4525	85
Model + nickel, *D* = 4 cm	381		4610	

Conclusion

From the performed investigations, we know that a change in the conductive material concentration cannot significantly reduce the temperature of the aluminum alloy but only delay its increase. This statement is true assuming specific spatial orientation of the filings of the conductive material in the protective layer.

The delay in the temperature increase on the surface of the aluminum alloy (orbiter structure) is of particular importance if the HRSI tiles are damaged. In extreme cases, it may even save the lives of the orbiter crew when returning to Earth where the destruction of the orbiter structure would take place after landing.

The additional conductive layer should be made from a material characterized by a high value of specific heat and high melting point. These properties may turn out useful not only for future orbital flights but perhaps also for interplanetary flights. Such a material should also have a relatively high density. During the research, nickel was a good candidate in this respect ensuring good insulator properties. For the adopted distribution of the heat flux for the two considered additions of nickel during the flight, the structure did not exceed its admissible operating temperature range, hence was not damaged. Moreover, the insulation with an additional material should ensure limited heat conduction towards the orbiter structure. It should also be characterized by a greater conduction in the transverse direction (compared to the main direction of the heat flux).

In the investigations, an improvement of the thermal properties of the insulator was obtained through increased thermal capacity of the material added to it. Hence, a greater efficiency of heat absorption was obtained – a limited heat flux to the protected inner layers. If there is a material loss due to a malfunction, the increase in the thermal capacity may be insufficient, which is why the transverse coefficient of heat conduction of the insulator was also increased. With relatively high material loss, the distance the heat needs to cover in order to penetrate the structure may be significantly reduced. This poses a risk of a quick damage of the structure. By increasing the transverse heat flux, the mechanism of accelerated heating of the lower insulator layers is inhibited. Such a property does not cause changes in the material that has not suffered any loss. In order to obtain such features, a material of special thermal properties was used and added to the insulator in the form of filings. The selection of the material, its location in the matrix of the LI900 primary material as well as the final thermal parameters was the subject of analysis in this paper.

Nomenclature

c – specific heat, [$\mathrm{Jkg^{-1}K^{-1}}$]
k – thermal conductivity, [$\mathrm{Wm^{-1}K^{-1}}$]
n – refractive index, [–]
q – heat flux density, [$\mathrm{Wm^{-2}}$]
s – optical thickness, [–]
T – temperature, [K]
t – time, [s]

Greek symbols

β – attenuation coefficient, [$\mathrm{m^{-1}}$]
γ – concentration of the addition, [%]
ε – thermal emissivity, [–]
κ_a – absorption coefficient, [–]
κ_s – scattering coefficient, [–]
ρ – density, [$\mathrm{kgm^{-3}}$]
σ – Stefan-Boltzmann constant, [$\mathrm{Wm^{-2}K^{-4}}$]

References

[1] Miller, J. E., *et al*., *Ballistic Performance of Porous-Ceramic*, American Institute of Physic, Shock Compression of Condensed Matter, Chicago, Ill., USA, 2011, Vol. 1426, pp. 84-87
[2] Wei, H. Ng., Thermomechanical Analysis of a Damaged Thermal Protection System, Ph. D. thesis, University of Michigan, Ann Arbor, Mich., USA, 2007
[3] Daryabeigi, K., *et al*., Heat Transfer Measurement and Modeling in Rigid High – Temperature Reusable Surface Insulation Tiles, NASA Technical Reports, Orlando, Fla., USA, 2011
[4] Kazemba, D. C., *et al*., Performance Characterization, Sensitivity and Comparison of a Dual Layer Thermal Protection System, *Proceedings*, 8th International Planetary Probe Workshop, Portsmouth, UK, 2011
[5] Grujicic, M., *et al*., Heat Transfer and Effective Thermal Conudtivity Analysis in Carbon-Based Foams for use in Thermal Protection Systems, *Journal of Materials Design and Applications*, *219* (2005), 4, pp. 217-230
[6] Mayers, E. D., *et al*., Parametric Weight Comparison of Advanced Metallic, Ceramic Tile, and Ceramic Blanket Thermal Protection Systems, NASA, Hampton, Va., USA, 2000
[7] Sukumaran, S., Anilkumar, S. H., Design and Analysis of Metallic Thermal Protection System (MTPS), *International Journal of Scientific and Research Publications*, 3 (2013), 2, pp. 483-488
[8] Zhu, H., Sankar, B. V., *Analysis of Sandwich TPS Panel with Functionally Graded foam Core by Galerkin in Method, Composite Structures*, Elsevier, Amsterdam, The Netherlands, 2007, Vol. 77, Issue 3, pp. 280-287
[9] Steeves, A. C., *et al*., A Magnetohydrodynamic Power Panel for Space Reentry Vehicles, *Journal of Applied Mechanics ASME*, *74* (2007), 1, pp. 57-64
[10] Yuen, W. W., *et al*., Combined Conductive/Radiative Heat Transfer in High Porosity Fibrous Insulation Materials: Theory and Experiment, *Proceedings*, 6th ASME –JSME Joint Thermophysics Conference, Kohala Coast, Hi., USA, 2003, pp. 201
[11] Balasubramaniam, R., Callister, S., *Materials Science and Engineering: Indian Adaptation*, Wiley India Pvt., Noida, India, 2009
[12] Dobrzanski, A. L., *Engineering Materials and Material Design. The Basics of Materials Science and Metallurgy*, Wydawnictwo Naukowo – Techniczne, Warsaw, Poland, 2006
[13] Wiliams, S. D., Curry, M. D., *Thermal Protection Materials-Thermophysical Property Data*, NASA, Houston, Tex., USA, 1992
[14] Byun, D., *et al*., Radiative Heat Transfer in Discretely Heated Irregular Geometry with an Absorbing, Emitting, and Anisortopically Scattering Medium using Combined Monte-Carlo and Finite Volume Method, *International Journal of Heat and Mass Transfer*, *47* (2004), 19-20, pp. 4195-4203
[15] Modest, M. F., *Radiative Heat Transfer*, 2nd edition, Academic Press, Amsterdam, The Netherlands, 2003
[16] Brunner, T. A., Forms of Application Transport, Sandia Report 2002-1778, Sandia National Laboratories, Albuquerque, N. Mex., USA, 2002
[17] Tarvainen, T., *et al*., *Coupled Radiative Transfer Equation and Diffusion Approximation Model for Photon Migration in Turbid Medium with Low-Scattering and Non-Scatterig Regions*, Institute of Phisics Publishing, Bristol, UK, 2005, Vol. 50, Issue 20, pp. 4913-4930

Paper submitted: November 29, 2018
Paper revised: December 28, 2018
Paper accepted: January 24, 2019